Fuzzy method for suppressing of different noises in color videos

Volodymyr Ponomaryov

Abstract— A novel approach in denoising of color videos corrupted by impulsive and additive noises is proposed. In difference with existing methods, novel method employs designed fuzzy rules selecting high similarity pixels in the vicinity of the central one using the correlation in the RGB channels and in the consecutive frames of a video for better preservation of the features via adjusting the possible local motions, processing separately the areas with different texture behaviors (e.g., smooth regions, edges, and fine details). Numerous simulation experiments have demonstrated the superiority of novel filters presenting better values for objective criteria (PSNR, MAE, NCD, SSIM) as well as in increasing the perceptual vision.

Keywords—Video, Fuzzy logic, Denoising, Similarity.

I. Introduction

The presence of noise produces deficiencies during acquisition, broadcast or storage of the color images and videos [1]-[-7]. Noise affects not only the performance of an image in a specific problem but also its perceived quality. Therefore, it is a priority task to filter each image or frame of a video prior to other processing in following stages [1]–[4], reducing the amount of noisy pixels. A principal problem here consists of a design of a noise reduction technique while image content (edges, fine features, etc.) should be preserved. Numerous techniques have been proposed that are mainly based on order statistics technique, on fuzzy logic theory, on sparse representation, etc. [8]–[19]. In color video filtering, employing existing interchannel and temporal correlation between the neighboring frames and processing them together it is possible to obtain sufficiently improved performance in comparison with case 2D frame filtering. The principal obstacle encountered when two or more frames are processed together for noise removal is the possible existence of local motions between different frames, which usually introduce motion blur and ghosting artifacts [14]-[17], [21]-[23]. Modern theoretical approaches in denoising of different noises are principally based on a possibility to gather more samples for similar parches in an image. Then, the methods use sophisticated statistical methods, which depend on image/noise model. The principal problem here is how to measure and employ the similarity of group of objects in a color image [20]-[28]. Proposed in this paper approach exploits the similar ideas using fuzzy set type filtering in searching similar parches that permit to gather more samples for processing together color channels for a video frame; following, more samples should be found gathering neighboring frames of a video where the local motions in different frames should be adjusted. The proposed approach in difference to other state-of-the-art approaches employs the RGB channels data and fuzzy logic description of semantic properties of image features via designed Fuzzy Rules in all filtering steps, processing several pixel gradients together in neighboring frames.

This work was supported by the Instituto Politécnico Nacional de Mexico and Consejo Nacional de Ciencia y Tecnología de Mexico.

Volodymyr Ponomaryov is with the Instituto Politécnico Nacional, ESIME-Culhuacan, Av. Santa Ana 1000, San Fco. Culhuacan, 04430, Mexico-city, Mexico (ph: 525556562058; fax: 525556562058 e-mail: vponomar@ipn.mx)

II. Fuzzy Approach in Denoising of Color Videos

In current paper, we present two novel techniques based on fuzzy logic approach in denoising: for impulsive noise suppression FMINS (*fuzzy multichannel impulse noise suppression*) filter, and for additive noise suppression FMANS (*fuzzy multichannel additive noise suppression*) filter.

A. Impulsive Noise Suppression

The designed method in denoising of impulsive noise is divided in three steps [16], [21]. In the first step, several gradient vector values for a basic gradient and four related gradients are computed. Each pixel is characterized by a level where it can be considered as *noise-free* and a level where it can be considered as *noisy*; the output of this step is denoted as $E(i,j)_1$. In the second step, the noise detection and filtering is based on mutual processing of three *RGB* color channels in a current frame. The output of the second stage is denoted as $E(i,j)_2$. In the final third step, the filtering procedure using spatial and temporal processing in two neighboring frames is performed where the remaining noisy pixels should be removed, guaranteeing edges and fine detail preservation, forming output filtering result $E(i,j)_3$. Details of FMINS framework are presented in the block diagram of Fig.1.

During filtering, a 3x3 sliding window located into a bigger 5x5 window in the novel framework is employed in present approach, applying the gradient values for neighboring pixels in eight different directions $\gamma = (NW, N, NE, E, SE, S, SW, W)$ with respect to a central pixel (see Fig.2).

$$\nabla^{\beta}_{(1,1)}E(i,j) = \nabla^{\beta}_{SE(B)}\,; \nabla^{\beta}_{(0,2)}E(i-1,j+1) = \nabla^{\beta}_{R1,\,SE}\,,$$
$$\nabla^{\beta}_{(2,0)}E(i+1,j-1) = \nabla^{\beta}_{R2,\,SE}\,, \qquad \nabla^{\beta}_{(-1,1)}E(i-1,j+1) = \nabla^{\beta}_{R3,\,SE}\,,$$
$$\nabla^{\beta}_{(1,-1)}E(i+1,j-1) = \nabla^{\beta}_{R4,\,SE} \qquad (1)$$

Two hypothesizes are resolved: the central pixel is a *noisy* or it is a *free-noise* pixel. The *LARGE* and *SMALL* fuzzy sets are introduced with an objective to estimate the noise contamination employing the Gaussian membership functions [6, 8] for membership degrees of gradient values [16]:

$$\rho\left(\nabla_{\gamma}^{\beta}, LARGE\right) = \begin{cases} 1, & \nabla_{\gamma}^{\beta} > \nabla_1 \\ \exp\left\{-\left[\left(\nabla_{\gamma}^{\beta} - \nabla_1\right)^2 / 2\sigma^2\right]\right\}, & otherwise \end{cases} \quad (2)$$

$$\rho\left(\nabla_{\gamma}^{\beta}, SMALL\right) = \begin{cases} 1, & \nabla_{\gamma}^{\beta} < \nabla_1 \\ \exp\left\{-\left[\left(\nabla_{\gamma}^{\beta} - \nabla_2\right)^2 / 2\sigma^2\right]\right\} & , otherwise \end{cases} . \quad (3)$$

The values of the parameters used in (2) and (3) were selected according to optimal values of *PSNR* and *MAE* criteria during several simulation experiments for different video sequences. The found values of these parameters are: $\nabla_1 = 60, \quad \nabla_{2,} = 9, \ \sigma^2 = 1000$; for interchannel RGB filtering $\nabla_{2,\text{inter}} = 9, \sigma^2_{\text{inter}} = 750;$ and in the case of mutual frames filtering: $\nabla_1 = 0.1, \quad \nabla_{2,} = 0.01, \ \sigma^2 = 0.1$ [16].

To resolve the hypothesis: a central pixel is *noisy* or *noise-free* that belongs to image features, several fuzzy rules are proposed. Table 1 exposes the designed fuzzy rules. *Fuzzy Rule 1-1* defines the fuzzy gradient value $\nabla_{\gamma}^{\eta F}$ that belongs to fuzzy set *LARGE* for *γ* direction. A color component pixel is considered as *noisy* pixel if its basic gradient value is similar to its related gradients R_3 and R_4, and differs from related gradients R_1 and R_2 (see Fig. 2). *Fuzzy Rule 1-2* presents the noisy factor r_{β} that gathers eight fuzzy gradient-directional values presented in the *Fuzzy Rule 1-1*. The noisy factor r_{β} is a measure to distinguish between a noisy pixel and a noise-free one. This value determines the level of noise presence in the processed sample in the fuzzy set *LARGE* indicating that this central pixel is corrupted. If a central pixel in a sliding window is considered as noisy one, the special procedure of ranking for all pixel values in ascending order according to its weights ρ_{γ}^{β} is used. Interchannel processing procedures that use the existing correlation between the *R*, *G* and *B* frame components are explained in the Fuzzy *Rules 2-1, 2-2* and *2-3* (Table 1). *Fuzzy Rule 2-1* defines the condition when the R component is *noise-free*. In final spatial-temporal stage, the remaining noisy pixels are now processed gathering data from two neighboring frames. The absolute difference values between (*t*) and (*t-1*) frames $\delta E_{(k,l)}^{\beta}$ are calculated, forming the error frame for time *(t)*. The remaining noisy pixels in this step are now processed inside a 5x5x2 sliding window, gathering two neighboring frames: $E^{t,\beta}(i,\ j)$, $E^{t-1,\beta}(i,\ j)$ calculating the difference values between (*t*) and (*t-1*) frames:

$$\delta E_{(k,l)}^{\beta} = \left| E^{t,\beta}\left(i+k, j+l\right) - E^{t-1,\beta}\left(i+k+k_1, j+l+l_1\right) \right| ,$$

$$k,l \in (-3,-2,-1,0,+1,+2,+3);\ k_1,l_1 \in (-1,0,-1);\ \beta = (R,G,B) \quad (4)$$

In this step, gradient values for frame difference $\nabla \delta_{\gamma(B\,or\,Ri)}^{\beta}$ for each of eight directions γ are used.

Additionally, the best match using criterion MAD should be found between the central pixel in current frame and pixels at the vicinity of of central one in previous frame, increasing size of common sample that consists of pixels from *(t)* and *(t-1)* frames. Finally, at postprocessing step, the complex (edges, fine details) and plane regions are processed separately (Fuzzy Rules: 3-1 to 3-4). *Fuzzy Rule 3-1* that employs the absolute difference gradient values $\nabla \delta_{\gamma}^{\beta}$ determines the first fuzzy gradient difference $\left(\nabla_{\gamma}^{\beta F}\right)_I$ for a central pixel in respect to its neighbors in a sliding window similar as it has been done in Fuzzy Rule 1-1. *Fuzzy Rule 3–2* determines the fuzzy gradient difference $\left(\nabla_{\gamma}^{\beta F}\right)_{II}$ using the fuzzy gradient differences in the direction γ, distinguishing between homogeneous and non-homogeneous regions. *Fuzzy Rule 3–3* computes the noisy factor r_{β} that gathers the fuzzy gradient-directional values presented in the Fuzzy Rule 3–1. *Fuzzy Rule 3–4* introduces the factor η_{β}.

B. Additive Noise Suppression

The designed method in denoising of additive noise uses similar *fuzzy ideology* of FMINS framework as it can be seen in the block diagram in Fig.3. There is used a *5x5* sliding window into bigger *7x7* sliding window to compute the gradient values in eight directions for basic and six related gradients (see Fig.2). The gradient values are introduced for each direction *γ* = {*N, E, S, W, NW, NE, SE, SW*}, where (*i, j*) values are {-3,-2,-1, 0, 1, 2, 3}. For FMANS filter, the *Fuzzy Rules 1-1* and *1-2*, where Gaussian functions are employed for calculating membership degrees of fuzzy gradient values, are used. In following stage of first step, the noise detection and filtering is based on mutual interchannel processing using RGB color representation in a current frame forming output of this stage. *Fuzzy Rule 1-3* defines the condition when the R component ca asn be estimated "*noise-free"*. *Fuzzy Rules 1-4* and *1-5* are employed to compute the weights for *noise-free* pixels as well as for *noisy* pixels. In next step, the filtering procedure is applied in spatio-temporal processing for two neighboring frames forming output filtering result (Fuzzy *Rules: 2-1 to 2-3*). The remaining noisy pixels in this step are now processed inside a 7x7x2 sliding window, gathering two neighboring frames: $E^{t,\beta}(i,\ j)$, $E^{t-1,\beta}(i,\ j)$ calculating the difference values between (*t*) and (*t-1*) frames (see eq. (4)). The best match using criterion MAD can be found between the central pixel in current frame and pixels at the vicinity of previous frame, increasing size of common sample that consists of pixels from *(t)* and *(t-1)* frames. Finally, at postprocessing step, the complex (edges, fine details) and plane regions are processed separately (*Fuzzy Rules: 3-1 to 3-3*) as presented in Table 2. Two variants of filtering are presented in Block diagram: FMANS_2 and FMANS_H, which uses hybrid processing connecting the "fuzzy ideology" of the FMANS technique and multiscale Wiener DCT-based filtering [28] is also performed that increases denoising ability as simulation results show.

III. Simulation Results and Performance Evaluation

The color videos *Flowers, Stefan, Foreman, Tennis* in the CIF format (352x288) and *Carphone, Grandma, Miss America and Saleman* in the QCIF format (176x144 pixels, RGB, 24 bits) [29] were used to evaluate the promising 3D fuzzy algorithms in wide range of impulsive noise intensity (0% to 20%). As shown in recently published articles the FRINR_Seq and 3D FD filtering techniques outperform all other existing state-of-the-art techniques in denoising impulsive noise, so comparing novel filter we justify in correct way the performance of novel FMINS 3D framework.

The filtered frames were evaluated according to PSNR (*Peak Signal-to-Noise Ratio*) that describes the noise suppression ability for an algorithm; the MAE (*Mean Absolute Error)* that measures the edge preservation ability [1-3], [5]. Additionally, another metric NCD (*Normalized Color Difference*, in the *L*u*v* color space) is used to measure color preservation properties of filtering results [2], [3]. Recently introduced SSIM (*Similarity Structural Index Measure*) [30] that matches better with human subjectivity is applied to characterize the performance of a chosen algorithm. These objective criteria and subjective perception via human vision are used to characterize the performance of the FMINS 3D filter averaging per 100 frames against mentioned techniques FRINR_Seq [17] and 3D-FD [15], [20], exposing the better values for *Foreman*, *Stefan*, *Grandma*, and *Carphone* color video sequences, guaranteeing its robustness. These results are exposed in Fig. 4a - 4c.

Table 5 presents the average per 100 frames *PSNR, MAE, NCD* and *SSIM* values for the proposed FMINS 3D framework against other better techniques FRINR_Seq and 3D FD, exposing the better values for *MA, SM, F,* and *S* video sequences. The best performance is realized by novel method according to all four objective criteria in wide range of noise intensity. Additionally, all three algorithms applied in filtering of the video sequences with varying the random impulse noise levels in range from 0% to 20%. The results of these experiments in terms of PSNR, MAE in different frames show that novel framework outperforms other better mentioned algorithms (Fig.4). The proposed fuzzy approach combines sufficiently good detail preservation to good noise removal and appear outperforms other compared filters in wide range of noise intensity.

Similar simulations on mentioned color videos have been performed in denoising of additive noise contamination. The proposed algorithm FMANS and other better techniques were evaluated in terms of the PSNR, MAE, NCD and SSIM criteria applied to different videos, presenting averaging values per 50 frames of each a video. As one can see in tables 5 and 6 the proposed (FMANS_2 and FMANS_H) techniques outperform other state-of-the-art techniques according to all criteria. The performance of the NLM is slightly better than for the other comparative filters. The FMANS_2 (window 7x7) and FMANS_H (Table 3) yield better results in comparison with the NLM, where the FMANS_H provides the best performance compared with all other denoising techniques. The same conclusion can be done analyzing behavior of criteria on different frames (see Fig.5).

Figure 6 shows the filtering frames and their error images for different filters in case of color video *Stefan*. In the 50th frame of the *Stefan* video, one can observe the better preservation of details in the field and letters located on the front wall compared with the other competing methods.

Comparing with the related state-of-the-art methods, the principal contributions of the current fuzzy approach are as follow:

- Developed fuzzy rules that permit selection of high similarity pixels in the vicinity of the central pixel employing the correlation in the RGB channels and in the consecutive frames of a video for better preservation of the features via adjusting the possible local motions.
- Separating and processing differently the areas with different texture behaviors (e.g., smooth regions, edges, and fine details).
- Hybrid denoising scheme for additive noise suppression that consists of combining the designed fuzzy framework and the multiscale Wiener filter at the final denoising stage.
- Preservation of the chromaticity properties of the image (such as color balance), avoiding unexpected color combinations after filtering operation.
- Demonstration of superiority in achieved better PSNR, MAE, NCD and SSIM values and in increasing the perceptual quality on the textured, and plain areas of the images.

Finally, while the proposed fuzzy approach is justified in the reduction of additive Gaussian and impulsive noises, nevertheless the fuzzy ideology can be generalized to other kind of noise because the filtering procedures adapt to the characteristics of an image without prior information, and it is also not necessary to have previous information about the type of noise that corrupts the image.

IV. Conclusion

The designed filters FMINS and FMANS are based on fuzzy logic approach using the interchannel correlations, matching possible motions in neighboring frames, forming the most similar pixels in different spatial areas of a current and neighboring frames of a video, finally, demonstrating superiority in comparison with better existing fuzzy and non fuzzy techniques in denoising of impulsive (FMINS) and additive (FMANS) noises.

These filters excellently suppress the noises in color videos, preserving edges, fine features, color properties, justifying their efficiency in PSNR, MAE, NCD and SSIM metrics and in subjective perception via human vision system.

Future work will be focused in increasing the ability of current fuzzy proposal in noise suppression for other kind of noises as well as in speed via parallel processing implementation on GPU hardware.

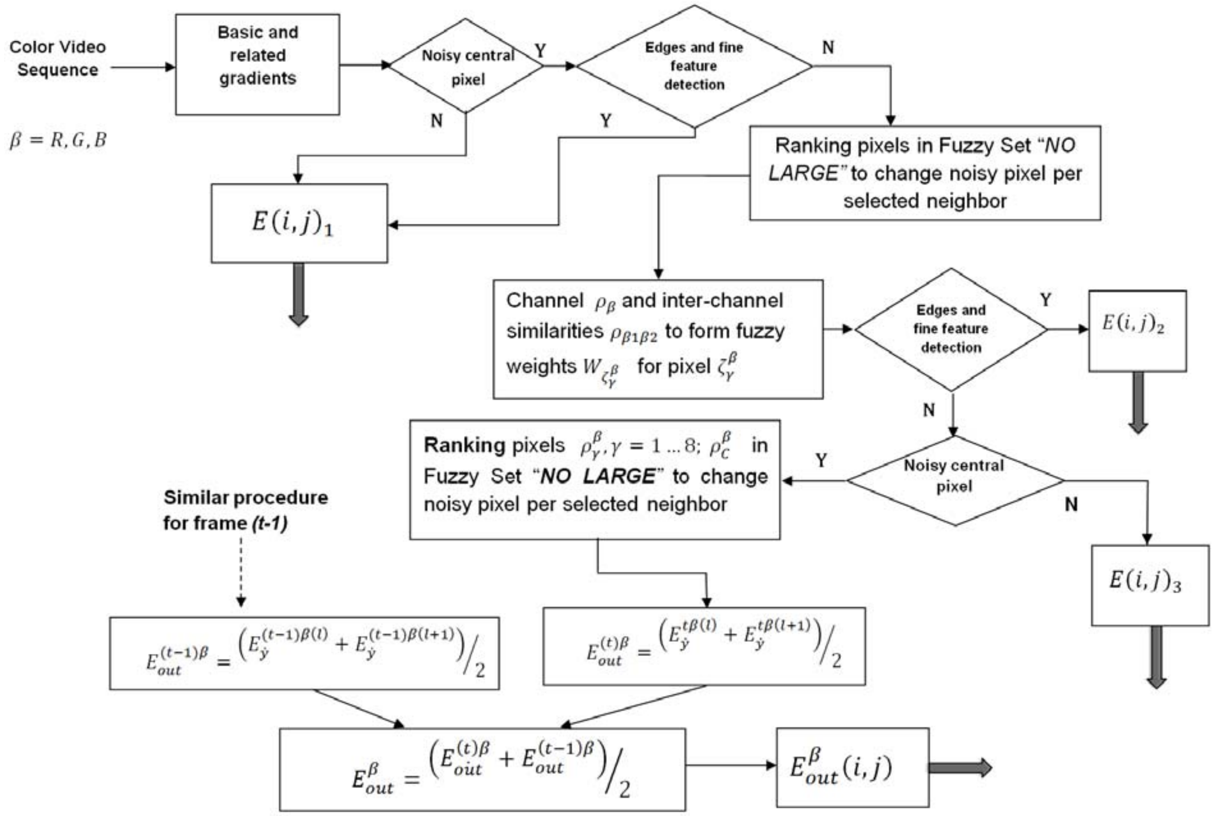

Fig. 1 Block diagram of FMINS denoising filter

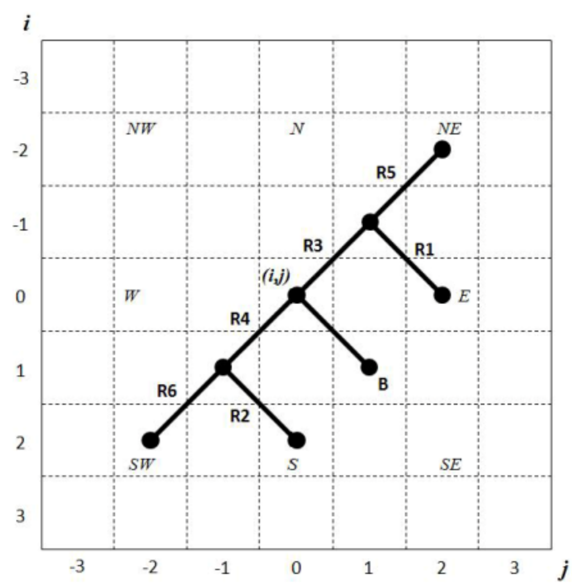

Fig.2 Basic B and several related (R_1 *to* R_6) gradients applied in sliding window

***FR 1-1**: Defining fuzzy gradient values* $\nabla_{\gamma}^{\beta F}$ into set LARGE	***IF** (* $\nabla_{\gamma B}^{\beta}$ *is L AND* $\nabla_{\gamma R1}^{\beta}$ *is S AND* $\nabla_{\gamma R2}^{\beta}$ *is S AND* $\nabla_{\gamma R3}^{\beta}$ *is L AND* $\nabla_{\gamma R4}^{\beta}$ *is L)* ***THEN Fuzzy Gradient*** $\nabla_{\gamma}^{\beta F}$ ***is LARGE**,* $(A\ AND\ B) = A \bullet B$ $(A\ OR\ B) = A + B - A \bullet B$.
***FR 1-2**: Defines fuzzy noisy factor* r_{β}	***IF MAX** (* ∇_{N}^{β} *is L,* ***MAX** (* ∇_{S}^{β} *is L,* ***MAX** (* ∇_{E}^{β} *is L,* ***MAX** (* ∇_{W}^{β} *is L,* ***MAX** (* ∇_{SW}^{β} *is L,* ***MAX** (* ∇_{NE}^{β} *is L,* ***MAX** (* ∇_{NW}^{β} *is L,* ∇_{SE}^{β} *is L)))))))* ***THEN*** r_{β} ***is LARGE**.*
***FR 2-1**: Membership degreee for R component* ς_{C}^{R} *in fuzzy set "noise free"* ***FR 2-2:** Defining the weight for R component* ς_{C}^{R}	***IF** (* μ^{R} *is L AND* μ^{RG} *is L AND* μ^{G} *is L) OR (* μ^{R} *is L AND* μ^{RB} *is L AND* μ^{B} *is L)* ***THEN*** *the noise-free degree* of ς_{C}^{R} ***is LARGE.*** ***IF*** $N(\varsigma_{C}^{R})$ *is LARGE* ***THEN*** $W(\varsigma_{C}^{R})$ ***is LARGE***
***FR 2-3**: Defining the weight* $W(\varsigma_{\gamma}^{R})$ *for the neighbor of R component* ς_{γ}^{R}	***IF*** ($N(\varsigma_{C}^{R})$ is not L AND $W(\varsigma_{\gamma}^{R})$ is L AND $\mu(\nabla\varsigma_{\gamma}^{G})$ is L AND $W(\varsigma_{\gamma}^{G})$ is L) OR ($N(\varsigma_{C}^{R})$ is not L AND $W(\varsigma_{\gamma}^{R})$ is L AND $\mu(\nabla\xi_{\gamma}^{B})$ is L AND $W(\varsigma_{\gamma}^{B})$ is L) ***THEN*** $W(\varsigma_{\gamma}^{R})$ ***is LARGE**.*
FR 3-1**: Determines the first fuzzy gradient difference* $\left(\nabla_{\gamma}^{\beta F}\right)_{I}$ *to characterize confidence "**movement-noise" ***FR 3-2.** Determines the fuzzy gradient difference* $\left(\nabla_{\gamma}^{\beta F}\right)_{II}$ ***FR 3-3** computes fuzzy factor fuzzy noisy factor* r_{β} *for interframe processing*	*Repeat **FR 1-1** changing* $\nabla_{\gamma B}^{\beta}$, $\nabla_{\gamma Ri}^{\beta}$ *,i=1,2,3,4 per* $\nabla\delta_{\gamma B}^{\beta}$, $\nabla\delta_{\gamma Ri}^{\beta}$ *, accordingly.* ***IF*** ($\nabla\delta_{\gamma B}^{\beta}$ is S AND $\nabla\delta_{\gamma R1}^{\beta}$ *is S AND* $\nabla\delta_{\gamma R2}^{\beta}$ *is S)* ***THEN*** $\left(\nabla_{\gamma}^{\beta F}\right)_{II}$ ***is SMALL*** *Repeat **FR 1-2** changing* ∇_{γ}^{β} *per* $\left(\nabla_{\gamma}^{\beta}\right)_{I}$
FR 3-4**: Determines the fuzzy factor* η_{β} *defining the confidence* ***"no movement-no noise" i*n interframe processing*	***IF MAX** (* $\left(\nabla_{N}^{\beta F}\right)_{II}$ *is S,* ***MAX** (* $\left(\nabla_{S}^{\beta F}\right)_{II}$ *is S,* ***MAX** (* $\left(\nabla_{E}^{\beta F}\right)_{II}$ *is S,* ***MAX*** *(* $\left(\nabla_{W}^{\beta F}\right)_{II}$ *is S,* ***MAX** (* $\left(\nabla_{SW}^{\beta F}\right)_{II}$ *is S,* ***MAX** (* $\left(\nabla_{NE}^{\beta F}\right)_{II}$ *is S,* ***MAX** (* $\left(\nabla_{NW}^{\beta F}\right)_{II}$ *is S,* $\left(\nabla_{SE}^{\beta F}\right)_{II}$ *is S)))))))* ***THEN*** η_{β} ***is SMALL**.*

Table.1 Fuzzy rules used in the FMINS filter

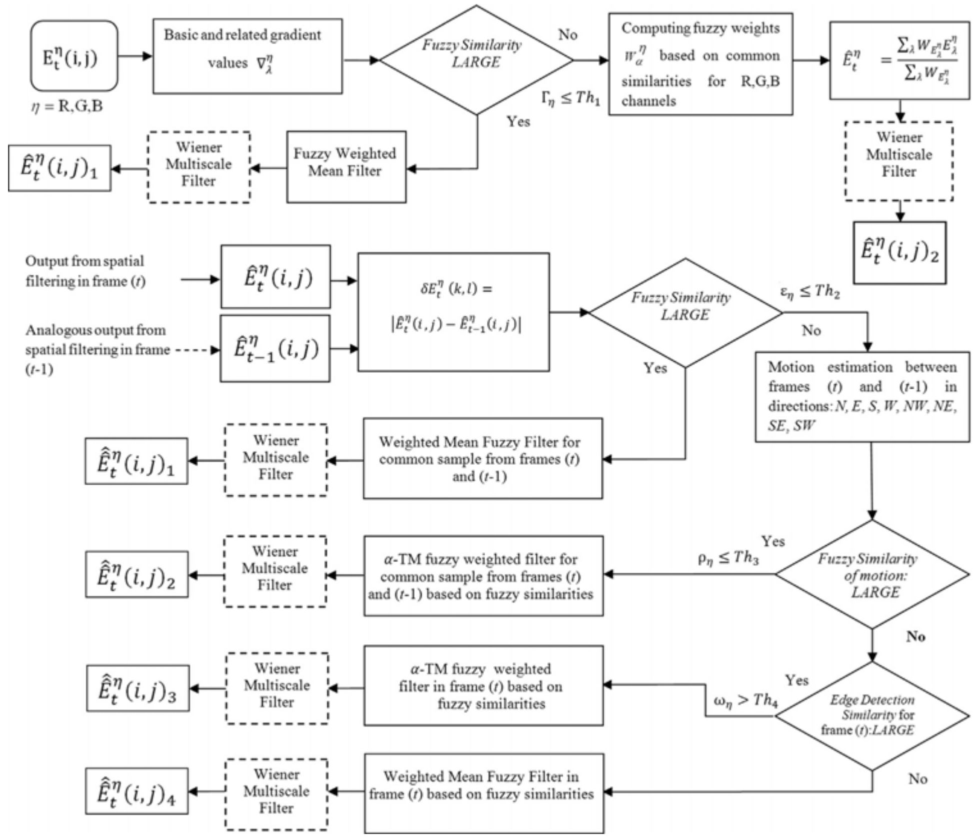

Fig.3 Block diagram of FMANS framework

Fuzzy Rule 1 − 1. *Defining the fuzzy gradient value $\nabla_\lambda^{\eta F}$ into the fuzzy similarity − set LARGE:*	**IF** $((\nabla_\lambda^\eta B$ is LARGE AND $\nabla_\lambda^\eta R1$ is LARGE$)$ OR $(\nabla_\lambda^\eta B$ is LARGE AND $\nabla_\lambda^\eta R2$ is LARGE$))$ AND $((\nabla_\lambda^\eta B$ is LARGE AND $\nabla_\lambda^\eta R3$ is LARGE$)$ OR $(\nabla_\lambda^\eta B$ is LARGE AND $\nabla_\lambda^\eta R4$ is LARGE$))$ AND $((\nabla_\lambda^\eta B$ is LARGE AND $\nabla_\lambda^\eta R5$ is LARGE$)$ OR $(\nabla_\lambda^\eta B$ is LARGE AND $\nabla_\lambda^\eta R6$ is LARGE$))$, **THEN** the fuzzy gradient value $\nabla_\lambda^{\eta F}$ is LARGE.
FuzzyRule 1 − 2. *Defining the fuzzy noisy factor Γ_η:*	**IF MAX**$((\nabla_N^\eta)$ is LARGE, **MAX**$((\nabla_S^\eta)$ is LARGE, **MAX**$((\nabla_E^\eta)$ is LARGE, **MAX**$((\nabla_W^\eta)$ is LARGE, **MAX**$((\nabla_{SW}^\eta)$ is LARGE, **MAX**$((\nabla_{NE}^\eta)$ is LARGE, **MAX**$((\nabla_{NW}^\eta)$ is LARGE, **MAX** $((\nabla_{SE}^\eta)$is LARGE$)))))))$, **THEN** the noisy factor Γ_η is LARGE.
Fuzzy Rule 1 − 3. *Defining the membership degrees $NE_{E_C^R}$ for the red component E_C^R in the fuzzy set "noise free":*	**IF**$(\tau^R$ is LARGE AND τ^{RG} is LARGE AND τ^G is LARGE$)$ OR $(\tau^R$ is LARGE AND τ^{RB} is LARGE AND τ^B is LARGE$)$, **THEN** the noise − free degree of E_C^R is LARGE, where the conjunction (A AND B) = A · B and the disjunction (A) OR (B) = A + B − A · B
Fuzzy Rule 1 − 4. *Defining the weight WE_C^R for the red component E_C^R:*	**IF** $(NE_{E_C^R}$ is LARGE$)$ **THEN** WE_C^R is LARGE.
Fuzzy Rule 1 − 5. *Defining the weight WE_λ^R for the neighbor of the red component E_λ^R:*	**IF** $(NE_{E_C^R}$ is NO LARGE AND $NE_{E_\lambda^R}$ is LARGE AND $\tau(\Delta E_\lambda^G)$ is LARGE AND $NE_{E_\lambda^G}$ is LARGE$)$ OR $(NE_{E_C^R}$ is NO LARGE AND $NE_{E_\lambda^R}$ is LARGE AND $\tau(\Delta E_\lambda^B)$ is LARGE AND $NE_{E_\lambda^B}$ is LARGE$)$, **THEN** $W_{E_\lambda^R}$ is LARGE.
Fuzzy Rule 2 − 1. *Defining the vectorial fuzzy gradient value $\nabla\delta E_\lambda^{\eta F}$ into the fuzzy −similarity set LARGE:*	**IF** $(\nabla\delta E_\lambda^\eta B$ is LARGE AND $\nabla\delta E_\lambda^\eta R1$ is LARGE$)$ OR $(\nabla\delta E_\lambda^\eta B$ is LARGE AND $\nabla\delta E_\lambda^\eta R2$ is LARGE$)$ AND $(\nabla\delta E_\lambda^\eta B$ is LARGE AND $\nabla\delta E_\lambda^\eta R3$ is LARGE$)$ OR $(\nabla\delta E_\lambda^\eta B$ is LARGE AND $\nabla\delta E_\lambda^\eta R4$ is LARGE$)$ AND $(\nabla\delta E_\lambda^\eta B$ is LARGE AND $\nabla\delta E_\lambda^\eta R5$ is LARGE$)$ OR $(\nabla\delta E_\lambda^\eta B$ is LARGE AND $\nabla\delta E_\lambda^\eta R6$ is LARGE$)$, **THEN** the fuzzy similarity value $\nabla\delta E_\lambda^{\eta F}$ is LARGE.
Fuzzy Rule 2 − 2. *Defining the fuzzy noisy factor ε_η:*	**IF** $($**MAX**$((\nabla\delta_N^\eta)$ is LARGE, **MAX**$((\nabla\delta_S^\eta)$ is LARGE, **MAX**$((\nabla\delta_E^\eta)$ is LARGE, **MAX**$((\nabla\delta_W^\eta)$ is LARGE, **MAX**$((\nabla\delta_{SW}^\eta)$ is LARGE, **MAX**$((\nabla\delta_{NE}^\eta)$ is LARGE, **MAX**$(\nabla\delta_{NW}^\eta$ is LARGE, $\nabla\delta_{SE}^\eta$ is LARGE$)))))))$, **THEN** the noisy factor ε_η is LARGE.
Fuzzy Rule 2 − 3. *Defining the weights for the Alfa − TM filter WE_λ in the case of motion for the central pixel located in (t) frame:*	**IF** $(NE_{E_C}$ is LARGE$)$, **THEN** WE_λ is LARGE.
Fuzzy Rule 3 − 1. *Defining the value of $\nabla_\lambda^{\eta F}$ for edges detection into the edge detection similarity − fuzzy set LARGE:*	**IF** $(\nabla_\lambda^\eta B$ is NO LARGE AND $\nabla_\lambda^\eta R1$ is NO LARGE$)$ OR $(\nabla_\lambda^\eta B$ is NO LARGE AND $\nabla_\lambda^\eta R2$ is NO LARGE$)$ AND $(\nabla_\lambda^\eta B$ is LARGE AND $\nabla_\lambda^\eta R3$ is LARGE$)$ OR $(\nabla_\lambda^\eta B$ is LARGE AND $\nabla_\lambda^\eta R4$ is LARGE$)$ AND $(\nabla_\lambda^\eta B$ is LARGE AND $\nabla_\lambda^\eta R5$ is LARGE$)$ OR $(\nabla_\lambda^\eta B$ is LARGE AND $\nabla_\lambda^\eta R6$ is LARGE$)$, **THEN** the fuzzy edge detection similarity gradient value $\nabla_\lambda^{\eta F}$ is LARGE.
Fuzzy Rule 3 − 2. *Defining the weights for the Alfa − TM filter WE_λ^R in the case of edge detection for the red component E_λ^R in the (t_{th}) frame:*	**IF** $(NE_{E_C^R}$ is LARGE$)$, **THEN** WE_C^R is LARGE.
Fuzzy Rule 3 − 3. *Defining the weights for the mean filter WE_C^R in the case of plain areas detection for the red component E_C^R in the (t_{th}) frame:*	**IF** $(NE_{E_C^R}$ is NO LARGE$)$, **THEN** WE_C^R is NO LARGE.

Table 2 Fuzzy rules used in FMANS filter

REFERENCES

1. Bovik, A., *Handbook of image and video processing (Communications, networking and multimedia)*, Orlando, FL, USA: Acad. Press Inc., 2005.
2. K. Plataniotis and A. Venetsanopoulos, *Color image processing and applications*, New York: Springer-Verlag, 2000.
3. R. Lukac, and K. N. Plataniotis, *Color Image Processing: Methods and Applications*, Boca Raton, FL, USA: CRC Press, 2006.
4. J. W. Woods, *Multidimensional Signal, Image, and Video Processing and Coding*, San Diego, CA, USA: Academic Press, 2011.
5. V. Kravchenko, H. Perez, V. Ponomaryov. *Adaptive Digital Processing of Multidimensional Signals with Applications*, Moscow: FizMatLit Edit., 2009. Available: http://www.posgrados.esimecu.ipn.mx/ (Libros publicados).
6. V. Ponomaryov. "Real-time 2D-3D filtering using order statics based algorithms," *J. Real Time Image Proc*., vol. 1, no.3, pp.173-194, 2007.
7. V.I Ponomaryov,. F.J. Gallegos-Funes, A. Rosales-Silva, "Real time color imaging based on RM-filters for impulsive noise reduction," *J. Imaging Sci. Technol.,* vol. 49, no.3, pp.205–219, 2005.
8. S. Morillas, V. Gregori, and A. Hervas, "Fuzzy Peer Groups for Reducing Mixed Gaussian-Impulse Noise From Color Images," *IEEE Trans. on Image Proc*., vol. 18, no. 7, pp.1452-1465, 2008.
9. C. Lien, C. Huang, P. Chen, Y. Lin, "An Efficient Denoising Architecture for Removal of Impulse Noise in Images," *IEEE Trans. on Comp.*, vol.62, no. 4, pp.631-643, 2013.
10. J. Varghese, M. Ghouse, S. Subash, M. Siddappa, M. S. Khan, O. B.Hussain, "Efficient adaptive fuzzy-based switching weighted average filter for the restoration of impulse corrupted digital images," *IET Image Process*., vol. 8, no. 4, pp.199-206, 2014.
11. J. Camarena, V. Gregori, S. Morillas and A. Sapena, "A simple fuzzy method to remove mixed Gaussian-impulsive noise from colour images," *IEEE Trans. Fuzzy Systems*, vol. 21, no.5, pp.971-978, 2013.
12. J.G. Camarena, V. Gregori, S. Morillas, A. Sapena, "Two-step fuzzy logic-based method for impulse noise detection in colour images," *Pattern Recogn. Lett*., vol. 31, no. 13, pp.1842-1849, 2010.
13. B. Smolka, "Peer group switching filter for impulse noise reduction in color images, *Pattern Recog. Lett*., vol. 31, no. 6, pp.484-495, 2010.
14. V. Ponomaryov, A. Rosales, F. Gallegos, "3D filtering of colour video sequences using fuzzy logic and vector order statistics," *Lecture Notes in computer Science*, vol. LNCS 5807, pp. 210–221, 2009.
15. V. Kravchenko, V Ponomaryov, V Pustovoit, "Three dimensional filtration of multichannel video sequences on the basis of fuzzy-set theory," *Doklady Phys.* Springer, vol. 55, no.2, pp.58–63, 2010.
16. V. Ponomaryov, H. Montenegro, A. Rosales, G. Duchen, "Fuzzy 3D filter for color video sequences contaminated by impulsive noise," *J. Real Time Image Proc.*, [Online]. Doi:10.1007/s11554-012-0262-9, pp.1-16, 2012.
17. T. Melange, M. Nachtegael and E. Kerre, "Fuzzy Random Impulse Noise Removal From Color Image Sequences," *IEEE Trans. on Image Processing,* vol. 20, no. 4, pp.959-970, 2011.
18. D. Fevralev, N. Ponomarenko, V. Lukin, S. Abramov, K.Egiazarian and J. Astola, "Efficiency analysis of color image filtering," EURASIP J. on Advances in Signal Processing, doi:10.1186/1687-6180-2011-41, 2011.
19. V. Ponomaryov, F. Gallegos-Funes, A. Rosales-Silva. Fuzzy directional (FD) filter to remove impulse noise from colour images. *IEICE Trans. Fund. Electron. Commun. Comput. Sci.*, vol.E93-A, no.2, pp.570–572, 2010.
20. A. Rosales-Silva, F. Gallegos Funes, V. Ponomaryov, "Fuzzy Directional (FD) Filter for impulse noise reduction in colour video sequences," *J. Visual Commun. & Image Represent*., vol. 23, no.1, pp.143-149, 2012.
21. L. Jovanov, A. Pizurica, A., A. Schulte, et. al., "Combined wavelet-domain and motion-compensated video denoising based on video codec motion estimation methods," *IEEE Trans. on Circ. Syst. Video Techn*., vol.9, no.3, pp.417-421, 2009.
22. T. Melange, M. Nachtegael, E, Kerre, "Video denoising by fuzzy motion and detail adaptive averaging," *J. Elect. Imag.,* vol.17, no.4, 043005, pp.1-19, 2008.
23. H. Yin, X. Fang, Z. Wei, and X Yang, "An Improved Motion-compensated 3-D LLMMSE filter with spatio-temporal adaptive filtering support," *IEEE Trans. on Circ. Syst. Video Tech*., vol.17, no12, pp.1714-1727, 2007.
24. M. Dong, J. W. Zhang, Y. Ma, "Image denoising via bivariate shrinkage function based on a new structure of dual contour let transform," *Signal Processing*, vol.109, pp.25-37, April, 2015.
25. A. Buades, B. Coll, and J., Morel, "A non-local algorithm for image denoising," in *IEEE Conf. Comput. Vis. Patt. Recogn,* vol. 2, pp.60-65, 2005.
26. K. Dabov, A. Foi, A., V. Katkovnik, and K. Egiazarian. Image denoising by sparse 3D transform-domain collaborative filtering", *IEEE Trans. Image Proces*., Vol.16, No.8, 2080-2095, 2007.
27. V. Ponomaryov, H. Montenegro-Monroy, L. Nino de Rivera, H. Castillejos, "Fuzzy Filtering Method for Color Videos Corrupted by Additive Noise," *The Scientific World Journal*, Vol. 2014, pp.1-21, Art. ID 758107.
28. O. Pogrebnyak,. V. Lukin, "Wiener discrete cosine transform-based image filtering," *J.f Elect. Imag., vol.*21, no. 4, paper 043020: pp.1-15, 2012.
29. Video Trace Library, http://trace.eas.asu.edu/yuv/, Arizona State University.
30. Z. Wang, A. and Bovik, "Mean squared error: love it or leave it? A new look at signal fidelity measures, *IEEE Sign. Proc. Mag*., vol.26, no.1, pp.98-117, 2009.

FMANS_H Algorithm

(a) Spatial Stage
1. **Input**: RGB video frame $E_t^\eta(i,j)$; where $\eta = R, G, B$.
2. Calculation of the Basic and related gradient values into a 7x7 sliding window $\nabla^\eta_{(k,l)}$.
3. *Fuzzy Similarity* set:

   if "LARGE"
   Weighted Mean Filter
   Wiener Multiscale Filter
   Output $\hat{E}_t^\eta(i,j)_1$
   else
   Fuzzy weights W_α^η are calculated.
   Weighted Mean Filter
   Wiener Multiscale Filter
   Output $\hat{E}_t^\eta(i,j)_2$

(b) Spatio-temporal denoising stage
1. **Input** *(t)and (t-1)* video frames
2. *Fuzzy Similarity* set is estimated $\delta E_t^\eta(i,j)$ in frames (*t*) and (*t-1*)
3. *Fuzzy Similarity* set:

   if "LARGE"
   Weighted Mean Filter for samples from (*t*) and (*t-1*) frames
   Wiener Multiscale Filter
   Output $\hat{\hat{E}}_t^\eta(i,j)_1$
   else
   Motion estimation between (*t*) and (*t-1*) frames in eight directions
4. *Fuzzy Similarity of motion* set:

   If "LARGE"
   Alfa-TM Filter for common samples from frames (*t*) and (*t-1*)
   Wiener Multiscale Filter
   Output $\hat{\hat{E}}_t^\eta(i,j)_2$
   else

(c) Fuzzy Spatial postprocessing Filtering Stage
1. *Edge Detection Similarity* set

   if "LARGE"
   Alfa-TM filtering is executed in frame (*t*)
   Output $\hat{\hat{E}}_t^\eta(i,j)_3$
   else
   Weighted Mean Filter in frame (*t*)
   Wiener Multiscale Filter
   Output $\hat{\hat{E}}_t^\eta(i,j)_4$

Table 3 Structure of FMANS_H algorithm

Volodymyr Ponomaryov attained his Ph.D. in 1974, D. Sci. in 1981. He is a referee for more than 20 international scientific journals. Dr. Ponomaryov served and currently serves as Associate Editor in *Journal of Real Time Image Processing* (Springer) His current research interests include signal/image and video processing, denoising, pattern recognition, real-time filtering, 3D reconstruction, medical sensors, remote sensing, etc. Over the years, he has also been a promoter of 39 Ph.D. degrees on his scientific areas of interests. He has authored or co-authored more than 150 scientific papers in the international referred journals, more than 300 international referred conference papers, and also 23 patents of ex USSR, Russia and Mexico, and five scientific books in international editorials.

Noise %	3D FD				FRINR_seq				FMINS			
	F		MA		F		MA		F		MA	
	PSNR	MAE	PSNR	MAE	PSNR	MAE	PSNR	MAE	PSNR	MAE	PSNR	MAE
0	30.46	1.68	48.22	0.037	30.99	1.47	49.62	0.022	**31.13**	**1.26**	**50.14**	**0.012**
5	29.41	2.13	39.36	0.381	30.26	1.95	39.75	0.369	**30.47**	**1.82**	**40.22**	**0.349**
10	28.46	2.72	35.99	0.752	29.97	2.25	36.52	0.716	**30.19**	**2.11**	**36.92**	**0.693**
20	26.84	4.16	32.10	1.826	27.21	3.84	32.65	1.610	**27.34**	**3.64**	**32.74**	**1.602**
	NCD	SSIM	NCD	SSIM	NCD	SSIM	NCD	SSIM	NCD	SSIM	NCD	SSIM
0	0.004	0.882	0.000	0.989	0.003	0.882	**0.000**	0.989	**0.002**	**0.883**	**0.000**	**0.9892**
5	0.005	0.847	0.002	0.982	0.005	0.849	0.001	0.982	**0.003**	**0.851**	**0.000**	**0.9824**
10	0.006	0.816	0.003	0.977	**0.005**	0.818	0.003	0.976	**0.005**	**0.820**	**0.001**	**0.977**
20	0.009	0.756	0.009	0.961	**0.007**	0.757	0.007	0.961.	**0.007**	**0.758**	**0.005**	**0.962**
Noise %	**3D FD**				**FRINR_Seq**				**FMINS**			
	S		**SM**		**S**		**SM**		**S**		**SM**	
	PSNR	**MAE**	**PSNR**	**MAE**	**PSNR**	**MAE**	**PSNR**	**MAE**	**PSNR**	**MAE**	**PSNR**	**MAE**
0	45.23	0.175	47.69	0.106	45.87	0.160	47.71	0.094	**46.33**	**0.152**	**47.94**	**0.083**
5	41.36	0.184	42.46	0.177	42.11	0.165	42.92	0.168	**43.11**	**0.158**	**43.67**	**0.156**
10	37.69	0.197	38.19	0.517	38.58	0.174	39.64	0.513	**38.82**	**0.168**	**40.27**	**0.505**
20	32.01	0.221	36.37	0.738	32.94	0.199	36.73	0.712	**33.11**	**0.188**	**37.12**	**0.702**
	NCD	**SSIM**	**NCD**	**SSIM**	**NCD**	**SSIM**	**NCD**	**SSIM**	NCD	SSIM	NCD	SSIM
0	0.009	0.986	0.003	0.962	0.007	0.993	0.002	0.962	**0.004**	**0.994**	**0.000**	**0.963**
5	0.010	0.959	0.006	0.931	0.009	0.973	0.004	0.930	**0.005**	**0.979**	**0.002**	**0.943**
10	0.013	0.941	0.009	0.909	0.011	0.952	0.007	0.915	**0.008**	**0.958**	**0.003**	**0.921**
20	0.019	0.913	0.012	0.872	0.012	0.907	0.009	0.874	**0.010**	**0.915**	**0.008**	**0.878**

Table.4 Mean per 100 frames values for *PSNR (dB)*, *MAE*, *NCD* and *SSIM* criteria (*F, MA, S* and *SM* video sequences)

Filters	**FDARTF_G** [5]		**VBM3D [26]**		**NLM [25]**		**FMANS_2**		**FMANS_H**	
Noise variance	**PSNR**	**MAE**	**PSNR**	**MAE**	**PSNR**	**MAE**	**PSNR**	**MAE**	**PSNR**	**MAE**
0.000	28.13	7.31	28.92	6.54	28.83	6.65	**29.38**	**6.39**	**29.71**	**6.21**
0.005	26.67	8.80	27.81	7.78	27.69	7.96	**28.17**	**7.54**	**28.51**	**7.38**
0.010	25.40	10.65	26.44	9.81	26.37	9.94	**26.83**	**9.65**	**27.09**	**9.39**
0.020	23.42	13.56	24.21	11.58	24.16	11.73	**24.58**	**11.33**	**24.95**	**11.17**
0.030	22.38	15.28	23.04	13.15	22.93	13.29	**23.37**	**12.96**	**23.75**	**12.64**
Noise variance	**NCD**	**SSIM**	**NCD**	**SSIM**	**NCD**	**SSIM**	**NCD**	**SSIM**	**NCD**	**SSIM**
0.000	0.014	0.8532	0.011	0.8869	0.011	0.8861	**0.011**	**0.8882**	**0.010**	**0.8896**
0.005	0.016	0.7975	0.015	0.8190	0.016	0.8179	**0.015**	**0.8192**	**0.013**	**0.8209**
0.010	0.023	0.7248	0.019	0.7515	0.019	0.7509	**0.019**	**0.7523**	**0.018**	**0.7542**
0.020	0.028	0.6395	0.020	0.6665	0.021	0.6659	**0.020**	**0.6672**	**0.019**	**0.6694**
0.030	0.031	0.6033	0.022	0.6319	0.023	0.6312	**0.022**	**0.6323**	**0.021**	**0.6338**

Table 5 Mean values per 50 video frames for criteria PSNR (dB), MAE, NCD, SSIM for color video Flowers after filtering

ISBN: 978-1-61804-285-9

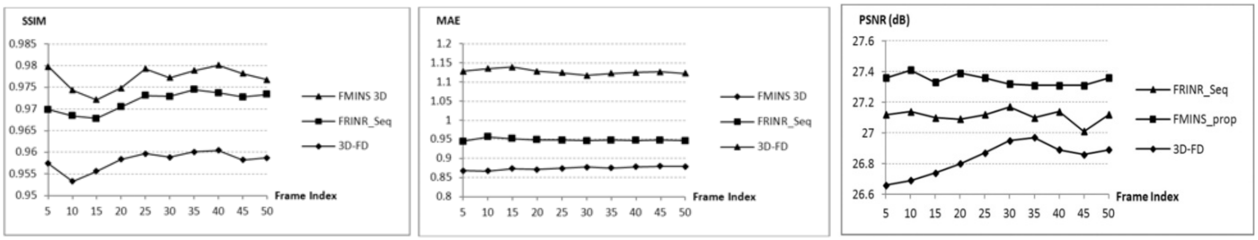

Fig.4 a) SSIM results for the different methods on *Stefan* video (p_n=5%). b) MAE results for the different methods on *Carphone* video (p_n=20%). c) PSNR results for the different methods on *Flowers* video (p_n=20%)

Filters	FDARTF_G [5]		VBM3D [26]		NLM [25]		FMANS_2		FMANS_H	
Noise variance	**PSNR**	**MAE**	**PSNR**	**MAE**	**PSNR**	**MAE**	**PSNR**	**MAE**	**PSNR**	**MAE**
0.000	35.68	5.36	36.46	4.74	36.39	4.82	***36.83***	***4.62***	**37.04**	**4.57**
0.005	33.25	7.70	34.41	7.07	34.38	7.21	***34.80***	***6.89***	**35.08**	**6.58**
0.010	31.69	9.70	32.53	8.79	32.41	8.88	***32.95***	***8.65***	**32.28**	**8.48**
0.020	28.84	11.31	29.65	10.62	29.57	10.69	***30.07***	***10.48***	**30.32**	**10.27**
0.030	26.26	12.82	27.39	12.03	27.32	12.14	***27.83***	***11.83***	**28.05**	**11.54**
Noise variance	**NCD**	**SSIM**	**NCD**	**SSIM**	**NCD**	**SSIM**	***NCD***	***SSIM***	**NCD**	**SSIM**
0.000	0.020	0.9454	0.018	0.9595	0.018	0.9586	***0.018***	***0.9611***	**0.017**	**0.9629**
0.005	0.022	0.8876	0.020	0.9005	0.021	0.8996	***0.019***	***0.9019***	**0.018**	**0.9047**
0.010	0.025	0.8279	0.022	0.8486	0.023	0.8472	***0.022***	***0.8498***	**0.021**	**0.8524**
0.020	0.030	0.7430	0.027	0.7721	0.028	0.7706	***0.026***	***0.7737***	**0.025**	**0.7761**
0.030	0.033	0.7074	0.029	0.7256	0.031	0.7241	***0.028***	***0.7271***	**0.026**	**0.7292**

Table 6 Mean values per 50 video frames for criteria PSNR (dB), MAE, NCD, SSIM for color video *Stefan* after filtering

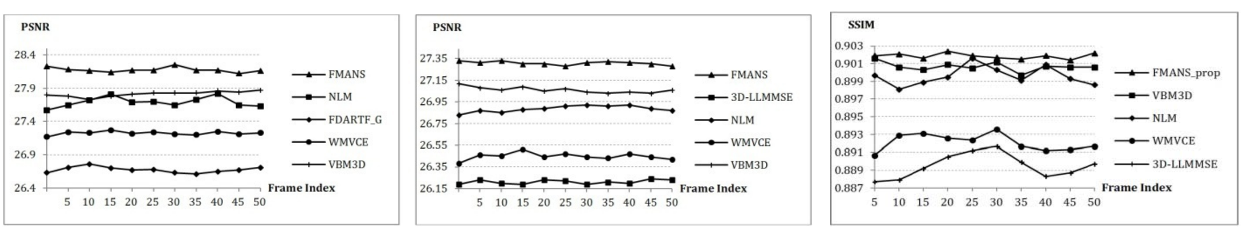

Fig.5a PSNR values for the different methods on *Tennis* video (σ^2 = 0.015) b) PSNR values for the different methods on *Stefan* video (σ^2 = 0.005) c) SSIM values for the different methods on *Stefan* video (variance 0.005)

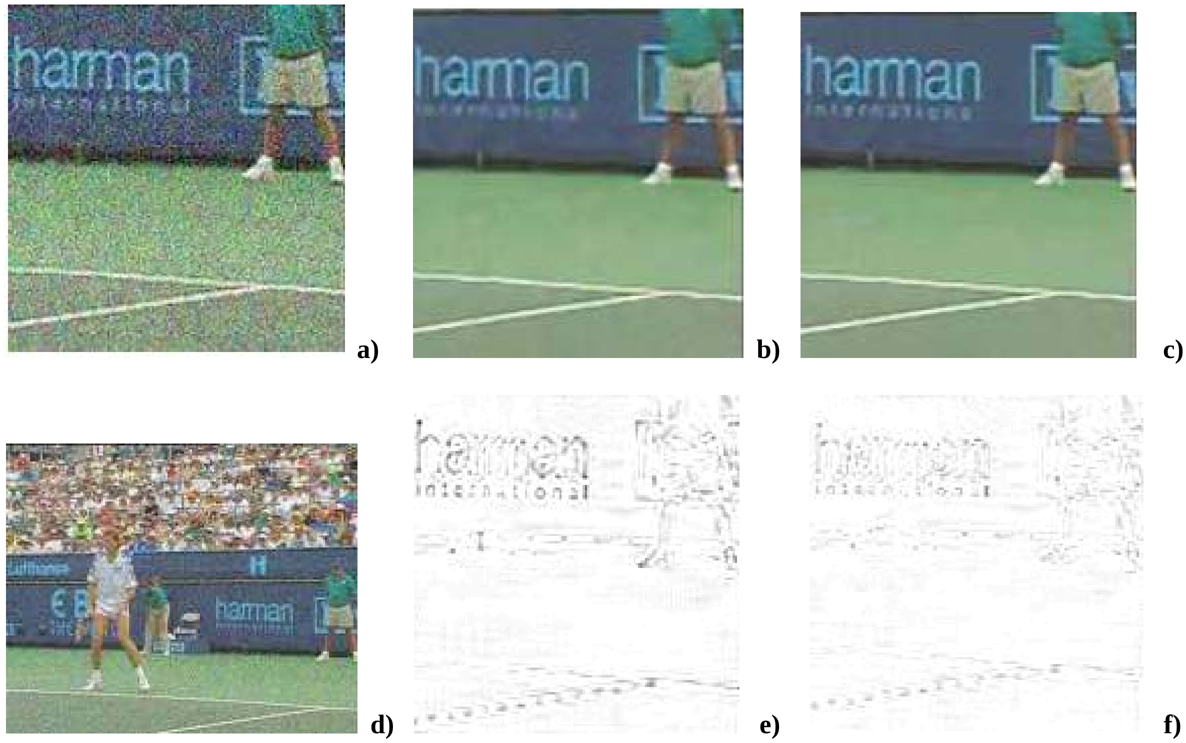

Fig. 6 (d) frame No.50 of color video *Stefan* contaminated by additive Gaussian noise with variance 0.02; a) zoomed part of contaminated frame, and filtered frames by: b) – *NLM*; c) –*FMANS_H*; e) and f) inverted error (amplified in 3 times) after filtering, accordingly for filters b) and c)

ISBN: 978-1-61804-285-9